

Boron–Nitrogen (BN) Substitution of Fullerenes: C₆₀ to C₁₂B₂₄N₂₄ CBN Ball

Jayasree Pattanayak, Tapas Kar,* and Steve Scheiner

Department of Chemistry and Biochemistry, Utah State University, Logan, Utah 84322-0300

Received: October 19, 2001; In Final Form: January 15, 2002

Semiempirical MNDO and density functional theory (B3LYP/3-21G) were used to examine the relative stability of the isomers of successive BN-substituted fullerenes C_{60-2x}(BN)_x, where $x = 1-24$. Doing so established certain rules of successive BN substitution in cage-like carbon materials. HOMO–LUMO gaps were also estimated for the entire series. It was found that heterofullerenes with less than 40% BN substitution have smaller band gaps than does semiconducting C₆₀.

Introduction

The discovery of fullerenes^{1,2} as stable structures of carbon has opened new research opportunities in science, engineering, and technology.³⁻⁶ Because boron and nitrogen bracket carbon in the periodic table, in their numbers of valence electrons, in their electronegativities, and in various other properties, attention has also been paid to alternate boron–nitrogen (BN) compounds.⁷⁻¹⁰ Pure BN is primarily found in a hexagonal h-BN (α -BN) form that resembles graphite, a sphalerite c-BN (β -BN) form related to cubic diamond, and a wurtzite-type γ -BN related to hexagonal diamond. Although the structural similarities between BN and analogous carbon compounds are strong, their physical, chemical, and electrical properties differ significantly. For example, graphite is an excellent host material and is semimetallic whereas, h-BN is an insulator with limited intercalation properties. Diamond is the hardest of all natural materials but is exceptionally unsuitable for the abrasion of iron materials and is oxidized at 700–900 °C in air, whereas c-BN is much more inert to iron and is stable up to 1600 °C in air, even though it has only half the hardness of diamond.

Properties intermediate between these two extremes, such as chemical inertness superior to that of diamond and hardness greater than that of c-BN, are expected in BCN materials where CC moieties of carbon compounds are partially substituted by BN units. It has also been predicted¹¹⁻¹⁶ that the doping of h-BN into graphite structure would alter its electronic properties. Heterofullerenes where one or more carbon atoms or pairs are substituted by boron, nitrogen, and BN pairs are gaining interest¹⁷⁻³⁶ as new hybrid materials. Several kinds of semiconductors can be expected from BCN materials. One is an intrinsic type of semiconductor that can be converted to a p-type or n-type extrinsic semiconductor by replacing C by B and N, respectively.

The single-BN-substituted C₆₀ molecule C₅₈BN has been examined by several groups^{22,35-37} using semiempirical approaches. Zhao and co-workers^{38,39} extended the study of BN-substituted fullerenes to trisubstitution by considering C_{60-2x}(BN)_x and C_{70-2x}(BN)_x ($x = 1-3$), using semiempirical AM1 and MNDO theories to predict their structures, stabilities, and electronic properties. The structure with a B–N bond between two hexagons is predicted to be most stable, compared to those

having the BN in a fusion position on a hexagon–pentagon border or those in which the B and N atoms are disconnected. They also found that the most stable structures contain the smallest numbers of B–C and N–C bonds.

Investigations of BN-substituted fullerenes have been further extended to substitution by as many as seven BN pairs in this laboratory⁴⁰ using semiempirical and DFT methods. The main objective of these investigations was to establish optimal BN substitution patterns in fullerene-like cage structures. The main findings of previous investigations are as follows: (i) isomers prefer to maximize the number of B–N bonds; (ii) stability is enhanced by keeping BN units together; and (iii) BN units first fill one hexagon then go on to adjacent hexagons, one by one, around a pentagon. Another ruling factor of successive BN substitution is the N-site attachment of the next BN unit to an existing group. Any other structural arrangements in which BN units are not consecutive, or some of the heteroatom pairs are placed in hexagon–pentagon joints, or a pentagon is filled cause instability. The same is true for an increase in the number of intervening rings between fully BN-substituted hexagons.

It has also been found⁴⁰ that the geometric parameters of C₆₀ are not much perturbed by BN substitutions, except in the immediate –BN–BN– region. Nitrogen atoms are bent slightly outward as a result of the presence of their lone pairs “inside” the cage structure. A wavelike or rippled surface of BN nanotubes in which B atoms are displaced inward and N atoms are moved outward has also been noted by Menon and Srivastava.⁴¹ Because of the electronegativity differences, the BN fullerenes acquire partial atomic charges in the heteroatom regions, the rest of the system remaining electrically neutral. The band gap of semiconducting C₆₀ is reduced by substitution, and the effect is more pronounced in partially filled or unsaturated⁴² BN fullerenes. The redox characteristics of C₆₀ also strongly depend on the number of BN units in C_{60-2x}(BN)_x.

In the present investigation, we continue to replace the –CC– units of C₄₆(BN)₇ (7-BN fullerene) all the way up to CBN ball (see Figure 1), C₁₂B₂₄N₂₄,^{25,31,35} where 24 pairs of carbon atoms are replaced by the isoelectronic BN moiety. It is worth mentioning that the positions of the 12 carbon atoms of C₁₂B₂₄N₂₄ are kept fixed during the substitution process. The substitution of any of these six carbon pairs will lead to a heterofullerene other than CBN ball. Although no evidence has yet been reported to demonstrate the stability of CBN ball, experimental works on BN-substituted cage-like structural forms

* Corresponding author. E-mail: tapaskar@cc.usu.edu. Tel.: 1-435-797-7230.

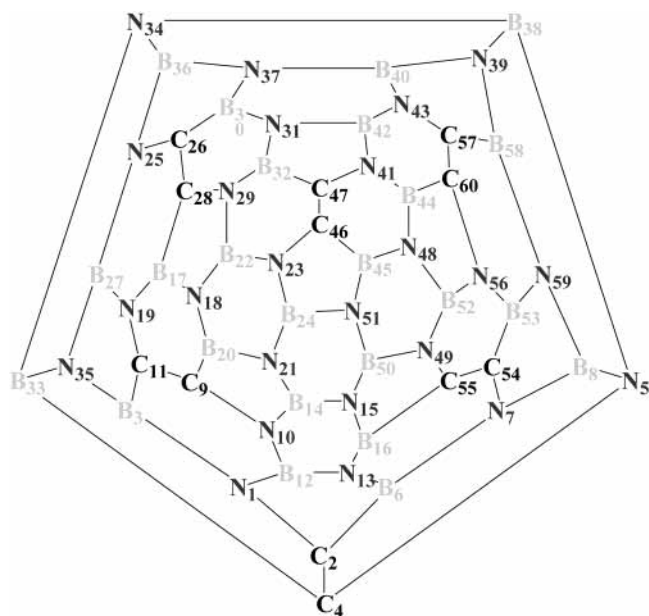


Figure 1. Schlegel diagrams of CBN ball ($C_{12}B_{24}N_{24}$).

of carbon materials are in progress.^{43,44} However, the arrangements of C, B, and N atoms in the BCN cage structures are not yet known. The heterofullerenes considered here cover a wide

range of BN concentrations (from 3.3 to 80%, including the most widely studied 50:50 combination of BN and C). Our main goal is to establish the successive substitution patterns in heterofullerenes. It will be interesting to explore whether the substitution patterns observed earlier are true also for higher BN concentrations and to identify any additional factor(s) that influence the higher degrees of BN replacement. Hybrid BCN systems have been synthesized by substituting carbon nano-materials.^{45–47} This synthetic method is a general substitution chemical reaction of carbon nanotubes during which C atoms are partially or completely substituted by B and N atoms without topological changes in the starting materials. Thus, the pattern of substitution might provide information on the growth of BN fullerenes from pure carbon systems. In addition to the structural arrangements, we also provide information on the electronic and chemical properties of BN-substituted fullerenes, as well as on the effect of successive substitution on those properties.

Method of Calculations

In the previous investigation⁴⁰ of 1–7-BN fullerenes, we found that, whereas quantitative aspects of relative energies are sensitive to different methods (namely, AM1, MNDO, B3LYP/3-21G//MNDO, B3LYP/3-21G//B3LYP/3-21G, PW91PW91/3-21G//PW91PW91/3-21G, and PW91PW91//MNDO), the trend is the same for all methods. On the basis of these findings, the

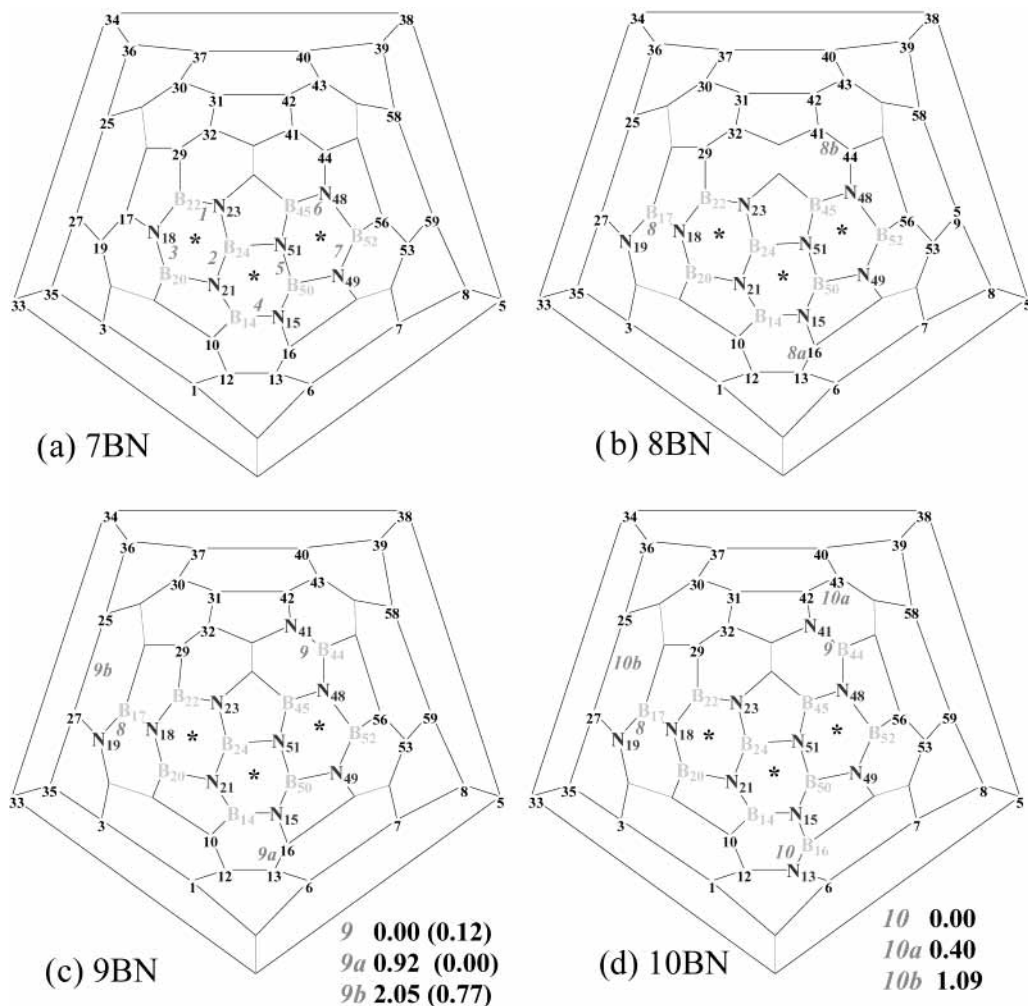


Figure 2. 7–10-BN fullerenes. The italic numbers indicate the order of BN substitution in sequence, and fully filled or saturated hexagons are marked with an asterisk (*). No number is assigned to those 12 C atoms that resist replacement. MNDO relative energies (E_{rel} in kcal/mol) of different isomers are also listed. Values in parentheses correspond to B3LYP/3-21G//MNDO energies. Relative energies of 8-BN fullerenes are summarized in Table 1.

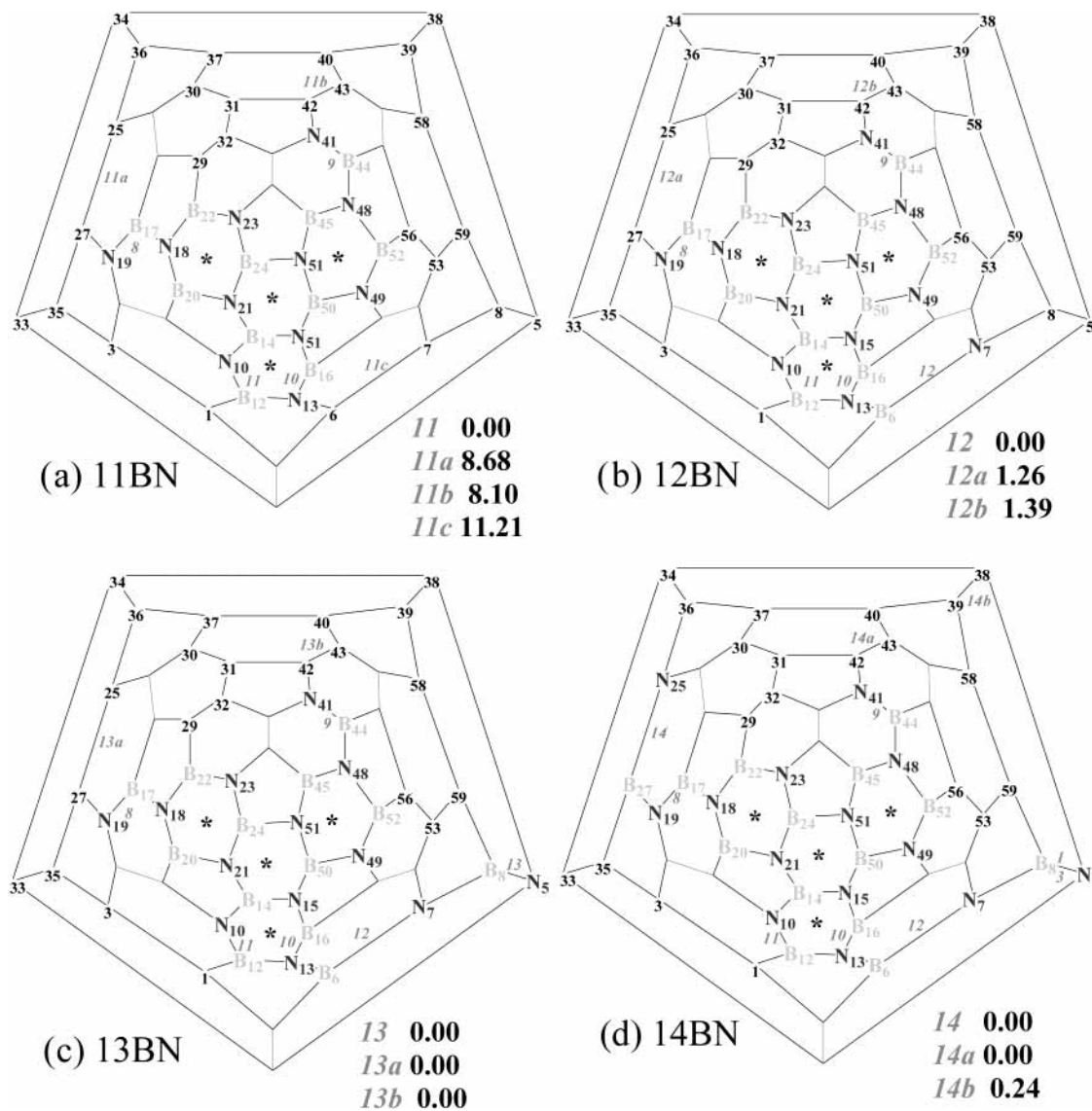


Figure 3. 11–14-BN fullererenes. The italic numbers indicate the order of BN substitution in sequence, and fully filled or saturated hexagons are marked with an asterisk (*). No number is assigned to those 12 C atoms that resist replacement. MNDO relative energies (E_{rel} in kcal/mol) of different isomers are also listed.

geometries of all systems were fully optimized without any symmetry constraints at the MNDO level. Vibrational analyses at the same level indicate that all isomers of 8–24-BN-substituted C_{60} considered in the present investigation have no imaginary frequencies, indicating true minima. Some of the isomers were also treated at the B3LYP/3-21G level. Finally, the properties of the most stable isomers of each group were calculated using the B3LYP/3-21G method. It is worth mentioning that, in this study, we are less interested in the absolute magnitudes of the energies or other properties than in their trends. Use of the B3LYP/3-21G method and MNDO geometries seems quite reliable for determining trends in electronic properties. For example, in the case of 1–7-BN fullererenes, the B3LYP/3-21G band gaps are only 4% larger than the B3LYP/6-31G* values, and this ratio is independent of the number of BN units in the heterofullerenes.

The bonding characteristics of the most stable isomers of C/BN fullererenes were examined using bond index analysis^{48–51} and Boys' localized molecular orbitals (LMOs)⁵² at the B3LYP/3-21G level. The positions of the charge centroids of the molecule were used to identify^{53,54} the bonds (two and three center) and lone pairs (LPs). Band gaps were estimated from

the energy difference between the highest occupied molecular orbital (HOMO) and the lowest unoccupied molecular orbital (LUMO). It is worth noting that, in DFT methods, these orbitals are best termed as Kohn–Sham (KS) orbitals. Recently, Stowasser and Hoffmann⁵⁵ showed that the shapes and symmetries of the KS orbitals are quite similar to those of the Hartree–Fock (HF) orbitals with which chemists are so familiar. The similarity between KS and HF orbitals has also been reported in several articles.^{56–58} These studies indicate that Koopmann's theorem, originally based on Hartree–Fock (HF) orbitals, can be extended to KS orbitals to estimate ionization potentials (IPs) and electron affinities (EAs). MNDO and DFT calculations were performed using the Gaussian 98 program.⁵⁹

Results and Discussion

For the sake of clarity, substitution patterns are illustrated via a Schlegel diagram, which essentially “flattens” the fullererenes into a two-dimensional plane. The order of BN substitution in 1–7-BN fullererenes is illustrated by the italic numbers in Figure 2a, each of which indicates a specific BN pair. For example, the first three CC pairs to be replaced are the 22–23, 21–24, and 18–20 pairs, filling a hexagon, as indicated by the asterisk.

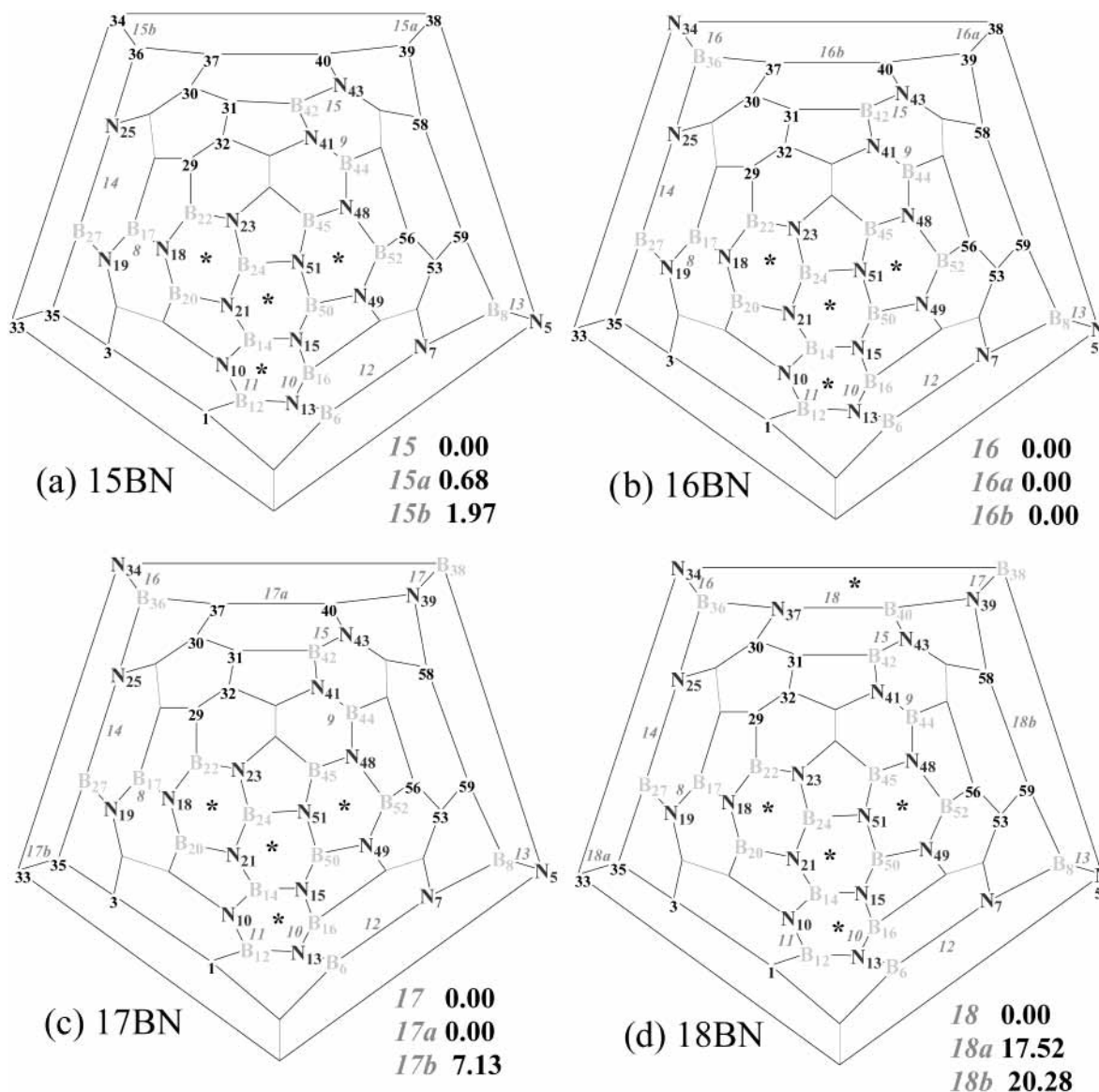


Figure 4. 15–18-BN fullerenes. Same notation as in Figure 3.

It can be seen that the first BN substitution takes place at a hexagon–hexagon junction and then spreads over to the same hexagon and adjacent two hexagons. Keeping not only B and N atoms but also BN units together enhances stability. The other crucial factor in BN substitution derived from our previous investigation is the preference for N-site attachment (N–BN) by the incoming BN group to the existing BN units. Keeping these substitution patterns in mind, we proceed to replace 8–24 carbon pairs of 7-BN fullerene to form $C_{12}B_{24}N_{24}$. The six carbon pairs of CBN ball (see Figure 1) are located on hexagon–hexagon (H–H) junctions, and thus, they connect 12 hexagons. The remaining eight hexagons of CBN ball are completely occupied by BN units. Thus, the presence of those 12 carbon atoms not only blocks some of the highly preferred H–H junctions for substitutions but also hinders the most favorable process of filling hexagons. These two restrictions, automatically generated by choosing CBN ball as the final target of successive BN substitutions from C_{60} , might lead to other minor or major patterns of substitution.

A. Substitution Sequences of BN Groups. 8–10-BN Fullerenes. Of the seven nitrogen atoms in 7-BN fullerene (Figure 2a), N_{21} and N_{51} are saturated (surrounded by three B atoms). Two other N atoms (N_{23} and N_{49}) are attached to one

of the 12 carbons of CBN ball (Figure 1) that are unlikely to be replaced because unfavorable^{17,35} B–B or N–N bonds would be the result. For example, replacement of the carbon pair in 46–47 by either B–N or N–B leads to a B_{45} – B_{46} or N_{23} – N_{46} bond, respectively. Replacement of any of the other five carbon pairs (55–54, 2–4, 9–11, 57–60, 26–28) of CBN ball at this stage will not result in a B–B or N–N bond, but eventually, such bonds will form as more and more substitution takes place. (Substitution of any one of these carbon pairs will lead to a completely different hybrid fullerene than CBN ball, and this is not the target of the present investigation.)

Thus, only three N atoms, namely, N_{15} , N_{18} , and N_{48} , of 7-BN fullerene are the active sites for next BN attachment. Relative energies (E_{rel}) of the three possible isomers **8**, **8a**, and **8b**, where the 8th BN unit is attached to N_{18} , N_{15} , and N_{48} , respectively, of 8-BN fullerene are reported in Table 1, and the isomers are shown in Figure 2b. (It should be noted that the B and N atoms are shown only for the most stable isomer **8** and that, for the less stable isomers, only the locations of the BN units are shown in Figure 2. This nomenclature is continued below.)

It can be seen from Table 1 that the trends in E_{rel} are the same for all methods. In general, **8** is the most stable followed by **8a** and **8b**. (Thus, the use of MNDO geometries seems quite

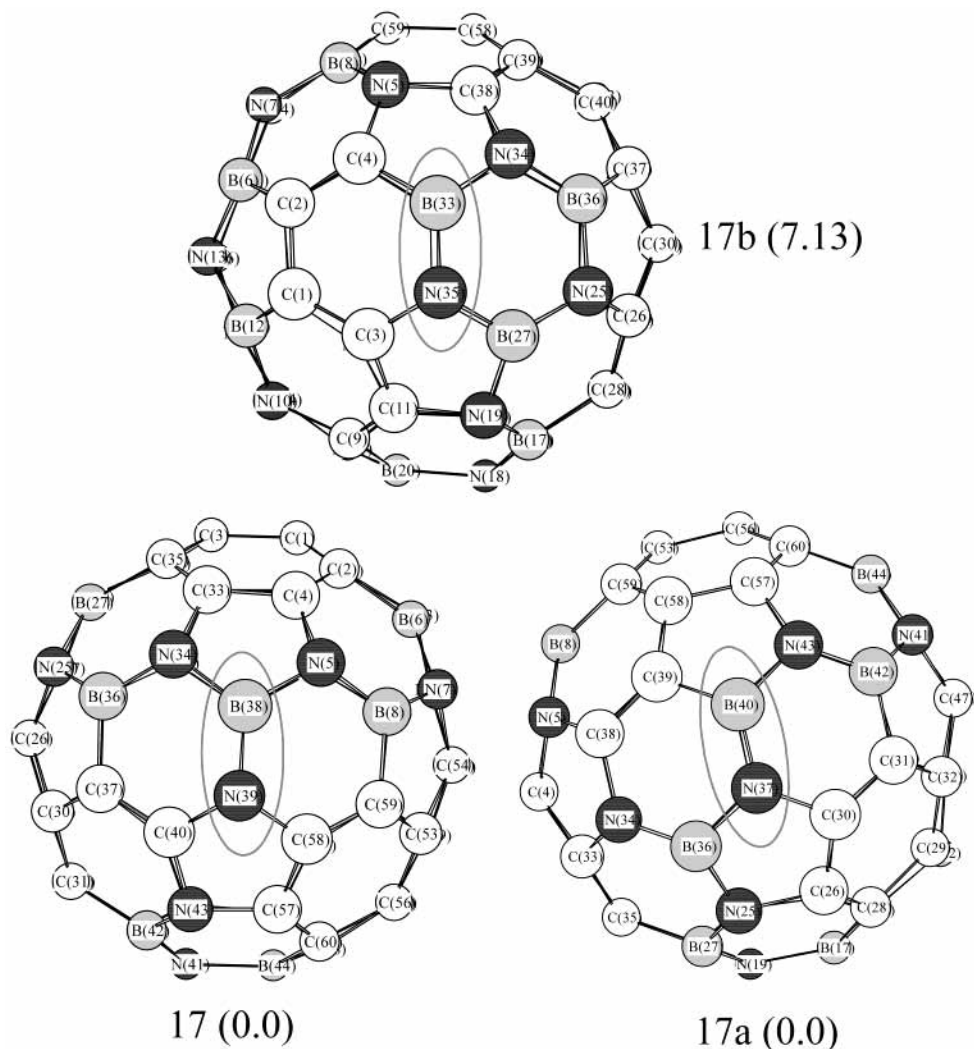


Figure 5. Three-dimensional diagram of the isomers of 17-BN fullerene. The position of the 17th BN unit is circled. Relative energies are given in parentheses.

TABLE 1: Relative Energies (E_{rel} , kcal/mol) and HOMO–LUMO Gaps (gap, eV) of 8-BN Fullerenes

method	E_{rel}			gap		
	8	8a	8b	8	8a	8b
MNDO/MNDO	0.00	2.85	2.64	6.51	6.61	6.40
B3LYP/3-21G//MNDO	0.00	1.80	3.28	2.87	2.98	2.61
B3LYP/3-21G//B3LYP/3-21G	0.00	1.70	3.28	2.90	3.00	2.66
B3LYP/6-31G**/B3LYP/3-21G	0.00	2.49	3.87	2.81	2.90	2.56
B3LYP/6-31G**/B3LYP/6-31G*	0.00	2.47	3.66	2.76	2.85	2.48

reasonable for these systems). Although it might initially appear that the hexagons involved in these three isomers are similar (each contains two BN and one CC units, and all three have the same number of B–N bonds), their environments are different. For example, the numbers of C, B, and N atoms in the surrounding hexagons and pentagons of the 18–17–19–11–9–20 hexagon (isomer **8**) are different from the numbers in the hexagons and pentagons surrounding the 45–48–44–41–47–46 hexagon (isomer **8b**). The main difference is related to the attached three pentagons, namely, 20–21–14–10–9 and 45–46–23–24–51. The former contains two carbons, one BN unit, and one B atom, whereas two BN units and one carbon atom constitute the latter pentagon. Similarly, one of the three surrounding hexagons of **8** and **8b** (i.e., 1–3–11–9–10–12 and 46–47–32–29–22–23, respectively) contains different numbers of constituent atoms. A close examination of the

geometrical parameters of 7-BN fullerene indicates that the C–C bond in the 17–19 position (1.373 Å) is shorter (perhaps because of its different location in the cage structure) than the C–C bonds at 44–41 (1.387 Å) and 13–16 (1.387 Å). The preference of BN substitution for shorter C–C bonds at hexagon–hexagon junctions over any other possible C–C junctions has already been observed in a previous investigation.⁴⁰ Thus, this confirms that the C–C distance is also a decisive factor for BN substitution. It should be noted that the isomers are all within 2–3 kcal/mol of each other.

A new substitution site (N₁₉) opens for 9-BN fullerene (Figure 2b), in addition to the left-over sites (N₁₅ and N₄₈) of 8-BN fullerene. (If the restrictions of fixing the positions of some carbon pairs were not imposed, C₁₁–C₉ would have been replaced to form the most stable 9-BN fullerene.) Isomers **9** and **9a** (Figure 2c) lie within 1.0 kcal/mol of one another and can be considered as essentially isoenergetic. At the DFT level, the relative energies are even closer to each other. Even less energy difference is found in isomers of 10-BN fullerene (Figure 2d). As in 8-BN fullerene, in both 9- and 10-BN fullerenes, hexagons involved in substitution contain one CC and two BN pairs and have the same number of B–N bonds. However, the replaced C–C bonds are of almost equal lengths (1.397–1.400 Å), so the preference of one site over the other is not obvious. Considering such small energy differences among these isomers (at higher levels of calculation, these difference might be further

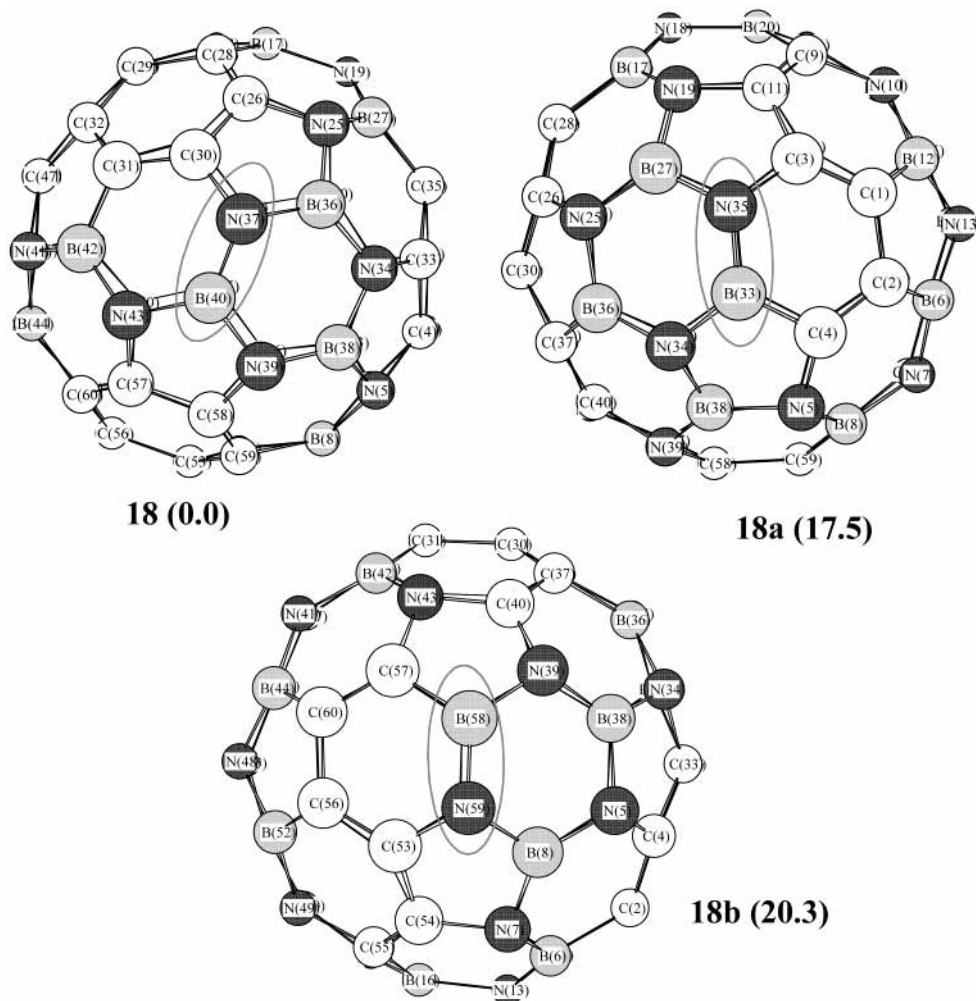


Figure 6. Three-dimensional diagram of the isomers of 18-BN fullerene. The position of the 18th BN unit is circled. Relative energies are given in parentheses.

lowered or reversed), it seems that the isomers of 9- and 10-BN fullerenes are equally preferred.

It is worth mentioning that the three open sites N_{18} , N_{48} , and N_{15} of 7-BN fullerene are filled first to form 8-, 9-, and 10-BN fullerenes, respectively, and each replacement of CC units by BN generates a new active N site, totaling three open sites for incoming BN groups. In general, this pattern of creating active sites after each BN substitution is common for the rest of the hybrid fullerenes.

11–16-BN Fullerenes. Four possible isomers of 11-BN fullerene are shown in Figure 3a. The nitrogen atom in position 13 generates the two isomers **11** and **11c**. It is quite obvious that isomer **11** is most stable because it contains a hexagon that is completely filled by three BN groups. The energy difference in this case is quite significant compared to previous BN fullerenes. It should be noted that, after 7-BN fullerene, the next completely filled hexagon is found in 11-BN fullerene.

The next substitution can take place at N_{13} , N_{19} , and N_{41} to form isomers **12**, **12a**, and **12b**, respectively. All of these isomers (Figure 3b) can be considered equally favorable because the energy difference is close to 1.0 kcal/mol. The energy difference diminishes for rest of the BN fullerenes considered in this subsection (see Figure 4 for 15- and 16-BN fullerenes). Considering these E_{rel} values, we conclude that multiple BN substitution might take place at the same time in these fullerenes. We have also attempted a different filling route by considering **13a** instead of **13** (not shown here) and filled up to 16-BN

fullerenes. This alternate substitution route eventually led to the same structural arrangement of 16-BN fullerenes.

17- and 18-BN Fullerenes. A completely new successive substitution pattern emerged from these two BN fullerenes. We saw earlier that filling of a hexagon enhances the stability of the isomer. This existing rule is overshadowed by the new pattern of substitution, which we term the “continuity rule”.

According to the hexagon filling rule, **17b** ($B_{33}N_{35}-B_{27}N_{25}-B_{36}N_{34}$ hexagon) ought to be the most stable isomer of 17-BN fullerene. However, **17b** is about 7.0 kcal/mol (6.4 kcal/mol at DFT/3-21G) more unstable than **17** and **17a**. To obtain a better view of the atomic arrangement, three-dimensional diagrams of these isomers, along with relative energies, are shown in Figure 5. The 17th BN unit in these isomers is also encircled for clear identification. It is clear from these figures that, in both **17** and **17a**, the 17th BN unit connects existing BN chains. Although these isomers contain the same number of B–N bonds, expanding the BN links causes extra stability. This extra stability is more clearly seen in 18-BN fullerene, as shown in Figure 6. In isomer **18**, the BN group not only completes the hexagon but also connects existing BN chains. These two ruling factors of BN substitution are the reason for the appreciable energy difference between **18** and **18a** or **18b**. The latter two isomers, in which hexagons are filled by BN groups, are close in energy.

19–24-BN Fullerenes. After 18-BN fullerene, six positions are left to complete the series. Of the six hexagons where the

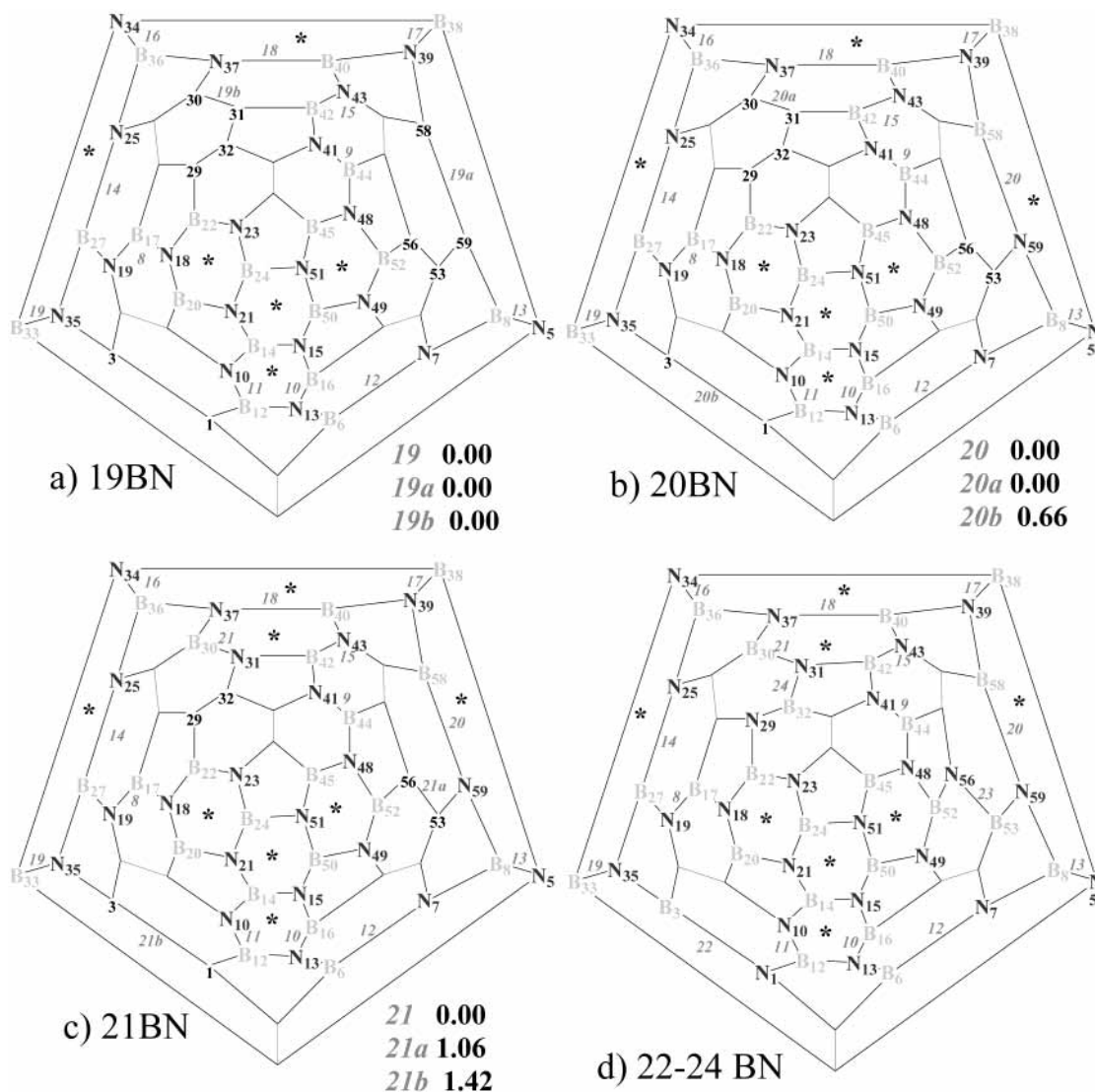


Figure 7. 19–24-BN fullerenes. Same notation as in Figure 3.

substitution positions are open, three contain one CC and two BN pairs, whereas the rest of the hexagons have one BN and two CC groups (see Figure 7). Because the stability of the isomers is enhanced by the filling of a hexagon, the former group is filled one by one, and then the second group is filled to finally form CBN ball. Isomers of these two groups are also isoenergetic.

In summary, the first three hexagons around a pentagon are filled one by one by BN groups to form 1–7-BN fullerene. The next three BN units attach to the existing units in such a way as to spread over the cage structure. One more hexagon is filled after this step, and once again, the next seven BN units occupy part of the seven hexagons. After substitution, each of these hexagons contains one CC and two BN units. Three BN units in a hexagon are found in 18–21-BN fullerenes. Thus, to this point, eight hexagons of C_{60} are completely filled by isoelectronic BN groups. It should be noted that exactly the same numbers of BN-filled hexagons are present in CBN ball. The remaining three hexagons with one BN and two CC units fill to form $C_{12}B_{24}N_{24}$. In most cases, the relative energies of the isomers are very close to each other, so the isomers can be considered isoenergetic.

B. Structure and Nature of Bonding. As in the case of 1–7-BN fullerenes, no multicenter bonds were found in 8–24-BN fullerenes. Localized molecular orbital (LMO) studies show that

electron pairs are perfectly localized on bonds and lone pairs (LPs) (not shown here; for more details, see ref 40). As expected, each pentagon–hexagon (P–H) connecting bond contains one electron pair, and two electron pairs are located between hexagon–hexagon (H–H) joints, causing different C–C bond lengths in C_{60} . Two different kinds of C–C bonds are found in heterofullerenes. These lengths are about 1.400 and 1.470 Å in H–H and P–H joints, respectively. Because of the presence of atoms with electronegativities different from that of C, these bonds deviate slightly from the above values. However, the effect of the number of BN groups in BN fullerenes on these bonds is not significant. All 12 C–C bonds in CBN ball contain two electron pairs and have bond lengths equal to 1.376 Å.

Unlike C–C bonds in hybrid fullerenes, B–N, B–C, and N–C bonds contain one bond pair, and nitrogen's lone pair is located inside the cage structure. As for C–C bonds, two different bond lengths are found for B–N bonds. The B–N bonds in H–H positions (1.450 ± 0.004 Å) are shorter than those located in H–P positions (1.485 ± 0.006 Å). The B–C and N–C bond lengths lie in the ranges 1.46–1.55 and 1.44–1.45 Å, respectively. In fact, successive BN substitution has little effect on the geometric parameters (except some angles). As in the case of small BC_2N molecules^{60,61} and 1–7-BN fullerenes,⁴⁰ sharper B–N–B and wider N–B–N bond angles are also associated with higher BN fullerenes. In general,

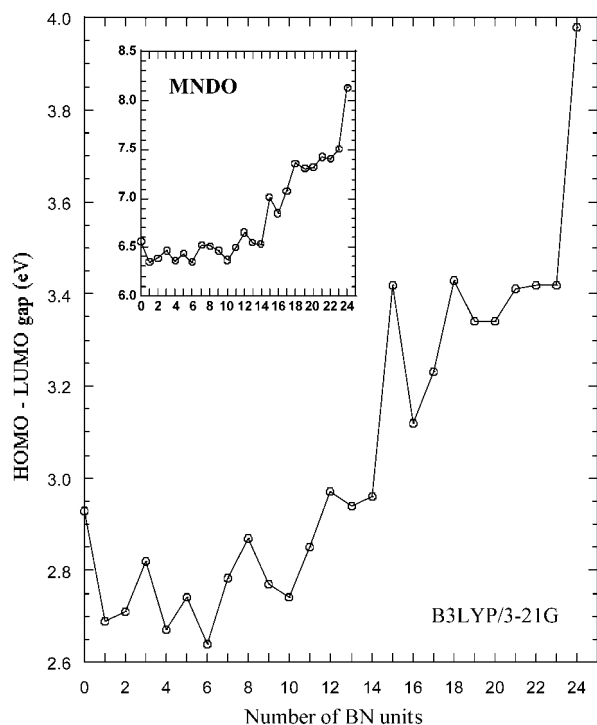


Figure 8. Variation in the HOMO–LUMO gap with number of BN groups.

B–N–B angles are significantly (more than 15°) different from 120° of $\theta(\text{C–C–C})$ in C_{60} , whereas the changes in other angles are within $3\text{--}5^\circ$.

C. HOMO–LUMO Gaps. For the sake of comparison and to show the complete series of BN fullerenes, the band gaps of $\text{C}_{60-2x}(\text{BN})_x$ ($x = 0\text{--}7$) obtained earlier⁴⁰ are also included in the figures in this section. Both DFT and MNDO gaps are plotted against the number of BN units in Figure 8. Although the HOMO–LUMO gap strongly depends on the method used, the trends are the same. In general, semiempirical gaps in the figure inset are about 2.2 times larger than the B3LYP/3-21G values. We also compared the HOMO–LUMO gaps of the three isomers of 8-BN fullerene using different methods, as shown in Table 1. Compared to B3LYP/6-31G**/B3LYP/6-31G*, the MNDO/MNDO values are 2.3–2.6 times higher, whereas other methods such as B3LYP/3-21G//MNDO or B3LYP/6-31G**/B3LYP/3-21G reproduce almost the same gap.

It is clear from Figure 8 that the band gap strongly depends on the number of BN units and that it follows a zigzag pattern through the series. Single BN substitution lowers the band gap of C_{60} by 0.24 eV at the DFT/3-21G level, and a slight increase (0.02 eV) is noticed upon addition of a second BN pair. In both cases, hexagons are partially filled by BN units. A sharp rise of 0.11 eV occurs when all three CC pairs of a hexagon are replaced by heteroatom pairs. This trend in the HOMO–LUMO gap also continues to higher BN fullerenes, reaching peaks for filled or saturated 5- and 7-BN fullerenes from their partially filled or unsaturated predecessor's gaps. The gap also depends on the number of BN-filled hexagons: it drops from 3- to 5-BN fullerene and then increases for 7-BN fullerene. In the case of unsaturated fullerenes, the gap goes down from 1- to 4- and then to 6-BN fullerene. Both methods predict the lowest gap for 6-BN fullerene.

Although a similar zigzag pattern is found for the band gaps of higher BN fullerenes, the dependence of this gap on the filling of BN units in hexagons is not strictly followed. For example, the gap of 11-BN fullerene, which contains four completely BN-

filled hexagons, is less than that of partially BN-filled 12-BN fullerene. On the other hand, 18-BN fullerene (five BN-filled hexagons) has a larger gap than its nearest saturated and unsaturated neighbors.

A significant discrepancy between the DFT and MNDO results was only encountered in the partially filled 8-BN fullerene. According to discussed trends in gaps, the MNDO value seems to obey the hexagon-filling rule. This erratic behavior of the band gap after 7-BN fullerene is due to the presence of carbon pairs on 12 hexagon–hexagon junctions. Nevertheless, it is clear from Figure 8 that 1–11-BN fullerenes (i.e., about 36% BN-substituted fullerenes) have smaller band gaps than semiconducting C_{60} . The rest of the BN fullerenes have larger gaps that increase with the number of BN units. It should be noted that the band gap of 15-BN fullerene, which is a 50:50 combination of carbon and BN, is significantly larger than that of C_{60} . This value is quite expected because the band gap of CBN ball (where 24 –CC– units are replaced by –BN– groups) is much larger than that of the parent C_{60} ⁶² and BN systems are well-known insulators.

Conclusion

To establish the pattern of successive substitution of carbon pairs of C_{60} fullerene by isoelectronic BN moieties, a large number of BN-substituted fullerenes (from C_{60} to CBN ball) have been considered using density functional and semiempirical theories. Although numerical values differ, trends in structure, stability, and electronic properties obtained using MNDO are in good agreement with more accurate DFT (B3LYP/3-21G) results.

A successive substitution pattern in the cagelike fullerene structures emerged from our present and previous investigations that includes the following general features:

(i) Carbon–Carbon Distance. BN substitution always prefers double-bonded sites rather than single-bonded carbon pairs. Thus, the carbon pair of any hexagon–hexagon (double-bond-type) junction of C_{60} is the first victim of BN substitution.

(ii) Hexagon-Filling Rule. BN units prefer to fill available consecutive hexagons. This pattern increases the number of B–N bonds. Thus, once the first substitution takes place, the next two BN units replace the carbons of the same hexagon. Further substitution spreads to adjacent hexagons one by one.

(iii) N-Site Attachment Rule. The incoming BN group always prefers to attach to an existing BN unit via BN–BN link. The other possible NB–NB is less favorable.

(iv) Continuity Rule. Joining existing BN chains spread over different hexagons significantly enhances the stability. This substitution pattern found in higher BN fullerenes, overrides the hexagon-filling rule.

In addition to the structural arrangements, we also estimated band gaps for the whole series. Depending on their band gaps, BN fullerenes are classified in two groups. The first group contains less than 40% BN units (i.e., 1–11-BN fullerenes), and their band gaps are smaller than that of semiconducting C_{60} . The rest of the cases, including the one with BC_2N stoichiometry, have larger gaps than C_{60} . In the former group, systems with completely filled hexagons have larger gaps than their partially filled neighbors. No such definite trend in band gaps is found for the second group of BN fullerenes.

BN units from 1- to 12-BN fullerene are spread in one hemisphere of the C_{60} , leaving the rest containing all carbon. The charge distributions in these two regions are different. Because of electronegativity differences, the BN-containing part of heterofullerenes acquires alternating charges, keeping the rest

of the C-containing region electrically neutral. The other important factor that we observed relates the locations of the nitrogen lone pairs. They are always inside the cage structure, and their locations are independent of the number of BN units.

References and Notes

- Bochvar, D. A.; Gal'pern, E. G. *Proc. Acad. Sci. USSR* **1973**, *209*, 239.
- Kroto, H. W.; Heath, J. R.; O'Brien, S. C.; Curl, R. F.; Smalley, R. E. *Nature* **1985**, *318*, 162–165.
- Dresselhaus, M. S.; Dresselhaus, G.; Eklunf, P. C. *Science of Fullerenes and Carbon Nanotubes*; Academic Press: New York, 1996.
- Kuzmany, H.; Fink, J.; Mehring, M.; Roth, S. *Fullerenes and Fullerene Nanostructures*; World Scientific: Singapore, 1996.
- Cioslowski, J. *Electronic Structure Calculations on Fullerenes and Their Derivatives*; Oxford University Press: New York, 1995.
- Hirsch, A. *Fullerenes and Related Structures*; Springer: Berlin, 1999; Vol. 199, p 246.
- Meller, A. *Gmelin Handbook of Inorganic Chemistry, Boron Compounds*; Springer-Verlag: Berlin, 1983; Vol. 1, 2nd Supplement.
- Meller, A. *Gmelin Handbook of Inorganic Chemistry, Boron Compounds*; Springer-Verlag: Berlin, 1988; Vol. 3, 3rd Supplement.
- Meller, A. *Gmelin Handbook of Inorganic Chemistry, Boron Compounds*; Springer-Verlag: Berlin, 1991; Vol. 3a, 4th Supplement.
- Paine, R. T.; Narula, C. K. *Chem. Rev.* **1990**, *90*, 73–91.
- Liu, A. Y.; Wentzcovitch, M.; Cohen, M. L. *Phys. Rev. B* **1989**, *39*, 1760–1765.
- Rubio, A.; Corkill, J. L.; Cohen, M. L. *Phys. Rev. B* **1994**, *49*, 5081–5084.
- Watanabe, M. O.; Itoh, S.; Mizushima, K.; Sasaki, T. *J. Appl. Phys.* **1995**, *78*, 2880–2882.
- Watanabe, M. O.; Sasaki, T.; Itoh, S.; Mizushima, K. *Thin Solid Films* **1996**, *282*, 334–336.
- Watanabe, M. O.; Itoh, S.; Mizushima, K.; Sasaki, T. *Appl. Phys. Lett.* **1996**, *68*, 2962–2964.
- Watanabe, M. O.; Itoh, S.; Sasaki, T.; Mizushima, K. *Phys. Rev. Lett.* **1996**, *77*, 187–189.
- Guo, T.; Jin, C.; Smalley, R. E. *J. Phys. Chem.* **1991**, *95*, 4948–4950.
- Miyamoto, Y.; Hamada, N.; Oshiyama, A.; Saito, S. *Phys. Rev. B* **1992**, *46*, 1749.
- Pradeep, T.; Vijayakrishna, V.; Santra, A. K.; Rao, C. N. R. *J. Phys. Chem.* **1991**, *95*, 1991.
- Piechota, J.; Byszewski, P.; Jablonski, R.; Antonova, K. *Fullerene Sci. Technol.* **1996**, *4*, 491–507.
- Chen, Z.; Zhao, X.; Tang, A. *J. Phys. Chem. A* **1999**, *103*, 10961–10968.
- Kurita, N.; Koboyashi, N.; Kumabara, H.; Tago, K.; Ozawa, K. *Chem. Phys. Lett.* **1992**, *198*, 95. Kurita, N.; Koboyashi, N.; Kumabara, H.; Tago, K. *Fullerene Sci. Technol.* **1993**, *1*, 319. Kurita, N.; Koboyashi, N.; Kumabara, H.; Tago, K. *Phys. Rev. B* **1993**, *48*, 4850.
- Wang, S. H.; Chen, F.; Fann, Y. C.; Kashani, M.; Malaty, M.; Jansen, S. A. *J. Phys. Chem.* **1995**, *99*, 6801.
- Chen, Z.; Reuther, U.; Hirsch, A.; Thiel, W. *J. Phys. Chem. A* **2001**, *105*, 8105–8110.
- Bowser, J. R.; Jelski, D. A.; George, T. F. *Inorg. Chem.* **1992**, *31*, 154–156.
- Jensen, F.; Toftlund, H. *Chem. Phys. Lett.* **1993**, *201*, 89–96.
- Jensen, H.; Sorensen, G. *Surf. Coat. Technol.* **1996**, *84*, 524–527.
- Silaghi-Dumitrescu, I.; Haiduc, I.; Sowerby, D. B. *Inorg. Chem.* **1993**, *32*, 3755–3758.
- Silaghi-Dumitrescu, I.; Lara-Ochoa, F.; Bishof, P.; Haiduc, I. *J. Mol. Struct. (THEOCHEM)* **1996**, *367*, 47–54.
- Brado, R. D.; T., S. C.; Jones, W. H. *Inorg. Chem.* **1994**, *31*, 154.
- Kabayashi, K.; Kurita, N. *Phys. Rev. Lett.* **1993**, *70*, 3542.
- Gao, Y. D.; Herndon, W. C. *J. Am. Chem. Soc.* **1993**, *115*, 8459.
- Placa, S. J. L.; Roland, P. A.; Wynne, J. J. *Chem. Phys. Lett.* **1992**, *190*, 163.
- Zhu, H.-Y.; Klein, D. J.; Seitz, W. A.; March, N. H. *Inorg. Chem.* **1995**, *34*, 1377–1383.
- Xia, X.; Jelski, D. A.; Bowser, J. R.; George, T. F. *J. Am. Chem. Soc.* **1992**, *114*, 6493–6496.
- Esfarjani, K.; Ohno, K.; Kawazoe, Y. *Phys. Rev. B* **1994**, *50*, 17830–17836.
- Chen, Z.; Ma, K.; Chen, L.; Zhao, H.; Pan, Y.; X., Z.; Tang, A.; Feng, J. *J. Mol. Struct. (THEOCHEM)* **1998**, *452*, 219–225.
- Chen, Z.; Ma, K.; Zhao, H.; Pan, Y.; Zhao, X.; Tang, A.; Feng, J. *J. Mol. Struct. (THEOCHEM)* **1999**, *466*, 127–135.
- Chen, Z.; Ma, K.; Pan, Y.; Zhao, X.; Tang, A. *J. Mol. Struct. (THEOCHEM)* **1999**, *490*, 61–68.
- Pattanayak, J.; Kar, T.; Scheiner, S. *J. Phys. Chem. A* **2001**, *105*, 8376–8384.
- Menon, M.; Srivastava, D. *Phys. Rev. Lett.* **1997**, *79*, 5086–5089.
- Hexagons containing three BN units are termed as saturated or fully filled. Otherwise, they are identified as partially filled or unsaturated. See ref 40 for details.
- Golberg, D.; Bando, Y.; Stephan, O.; Bourgeois, L.; Kurashima, K.; Sasaki, T.; Sato, T.; Goringe, C. *Jpn. Soc. Electron Microsc.* **1999**, *48*, 701–709.
- Golberg, D.; Bando, Y.; Stephan, O.; Kurashima, K.; Sasaki, T.; Sato, T.; Goringe, C. New Fullerenes in the C–B–N System Formed through Electron Irradiation Induced Solid State Phase Transformation; In *Solid State Phase Transformations*; Koiwa, M., Otsuka, K., Miyazaki, T., Ed.; The Japan Institute of Metals: Sendai, Japan, 1999; pp 1301–1304.
- Han, W. Q.; Bando, Y.; Kurashima, K.; Sato, T. *Appl. Phys. Lett.* **1998**, *73*, 3085–3087.
- Han, W. Q.; Bando, Y.; Kurashima, K.; Sato, T. *Chem. Phys. Lett.* **1999**, *299*, 368–373.
- Golberg, D.; Bando, Y.; Han, W.; Kurashima, K.; Sato, T. *Chem. Phys. Lett.* **1999**, *308*, 337–342.
- Sannigrahi, A. B. *Adv. Quantum Chem.* **1991**, *23*, 301–351.
- Sannigrahi, A. B.; Kar, T. *Chem. Phys. Lett.* **1990**, *173*, 569–572.
- Kar, T.; Marcos, E. S. *Chem. Phys. Lett.* **1992**, *192*, 14–20.
- Kar, T. *J. Mol. Struct. (THEOCHEM)* **1993**, *283*, 313–315.
- Boys, S. F. *Quantum Theory of Atoms, Molecules and the Solid State*; Academic Press: New York, 1966.
- Kar, T.; Jug, K. *Chem. Phys. Lett.* **1996**, *256*, 201–206.
- Kar, T.; Jug, K. *Int. J. Quantum Chem.* **1995**, *53*, 407.
- Stowasser, R.; Hoffmann, R. *J. Am. Chem. Soc.* **1999**, *121*, 3414.
- Yang, W.; Mortier, W. J. *J. Am. Chem. Soc.* **1986**, *108*, 5708.
- Hoffmann, R. *J. Mol. Struct. (THEOCHEM)* **1998**, *424*, 1.
- Kar, T.; Angyan, J. G.; Sannigrahi, A. B. *J. Phys. Chem.* **2000**, *104*, 9953–9963.
- Frisch, M. J.; Trucks, H. B.; Schlegel, G. W.; Scuseria, G. E.; Robb, M. A.; Cheeseman, J. R.; Zakrzewski, V. G.; Montgomery, J. J. A.; Stratmann, R. E.; Burant, J. C.; Dapprich, S.; Millam, J. M.; Daniels, A. D.; Kudin, K. N.; Strain, M. C.; Farkas, O.; Tomasi, J.; Barone, V.; Cossi, M.; Cammi, R.; Mennucci, B.; Pomelli, C.; Adamo, C.; Clifford, S.; Ochterski, J.; Petersson, G. A.; Ayala, P. Y.; Cui, Q.; Morokuma, K.; Malick, D. K.; Rabuck, A. D.; Raghavachari, K.; Foresman, J. B.; Cioslowski, J.; Ortiz, J. V.; Baboul, A. G.; Stefanov, B. B.; Liu, G.; Liashenko, A.; Piskorz, P.; Komaromi, I.; Gomperts, R.; Martin, R. L.; Fox, D. J.; Keith, T.; Al-Laham, M. A.; Peng, C. Y.; Nanayakkara, A.; Gonzalez, C.; Challacombe, M.; Gill, P. M. W.; Johnson, B.; Chen, W.; Wong, M. W.; Andres, J. L.; Gonzalez, C.; Head-Gordon, M.; Replogle, E. S.; Pople, J. A. *Gaussian 98*, revision A.7; Gaussian, Inc.: Pittsburgh, PA, 1998.
- Kar, T.; Cuma, M.; Scheiner, S. *J. Phys. Chem. A* **1998**, *102*, 10134–10141.
- Kar, T.; Cuma, M.; Scheiner, S. *J. Mol. Struct. (THEOCHEM)* **2000**, *556*, 275–281.
- Kobayashi, K.; Kurita, N. *Phys. Rev. Lett.* **1993**, *70*, 3542–3544.